



**Environmental  
Science**  
Water Research & Technology

**Treatment of Brackish Water Inland Desalination Brine via  
Antiscalant Removal Using Persulfate Photolysis**

Journal:	<i>Environmental Science: Water Research &amp; Technology</i>
Manuscript ID	EW-ART-12-2022-000924.R1
Article Type:	Paper

SCHOLARONE™  
Manuscripts

### **Water Impact Statement**

Brine disposal remains a challenge for inland brackish water desalination due to the cost and negative environmental impacts. This study developed the combined persulfate photolysis and chemical demineralization process to effectively treat brine. Implementing the suggested process has the potential to improve the sustainability of inland desalination by reducing the brine volume and its negative environmental impact.

# **Treatment of Brackish Water Inland Desalination Brine via Antiscalant Removal Using Persulfate Photolysis**

Soyoon Kum<sup>1,2</sup>, Xinyu Tang<sup>1</sup>, and Haizhou Liu<sup>1\*</sup>

<sup>1</sup>Department of Chemical and Environmental Engineering, University of California at Riverside,  
Riverside, CA 92521 USA

<sup>2</sup>Current address: David L. Hirschfeld Department of Engineering, Angelo State University, San  
Angelo, TX 76909 USA

\* Corresponding author, e-mail: [haizhou@engr.ucr.edu](mailto:haizhou@engr.ucr.edu)

phone (951) 827-2076, fax (951) 827-5696

*Submitted to Environmental Science: Water Research & Technology*

**Abstract**

Brine disposal is a challenging issue for brackish water desalination in inland regions. This study developed an ultraviolet-driven persulfate oxidation pre-treatment (UV/PS) followed by a chemical demineralization (CDM) and microfiltration to effectively treat brackish water desalination brine, specifically by degrading antiscalant during UV/PS and precipitating scale-forming calcium from the brine during CDM. To optimize calcium removal kinetics, the effects of persulfate dose and UV irradiation time during UV/PS were investigated and softening by NaOH and lime during CDM were evaluated. UV/PS pre-treatment successfully eliminated the scale inhibition effect of antiscalant, resulting in an enhanced chemical demineralization performance. A few minutes of CDM operating time was sufficient to remove more than 85% of total calcium from the brine due to the fast sedimentation of calcium precipitates. Moreover, compared to a control (no pre-treatment), the subsequent microfiltration (MF) membrane fouling potential was reduced by 80%. Overall, the application of the UV/PS-CDM-MF combined process has the potential to remove more than 90% of calcium from the brackish desalination brine, and consequently recover a significant amount of fresh water (>90%) from the brine. Results from this study point to UV/PS-CDM process as a promising brine treatment technology to remove scale-forming precursors and improve water recovery.

**Water Impact Statement**

Brine disposal remains a challenge for inland brackish water desalination due to the cost and negative environmental impacts. This study developed the combined persulfate photolysis and chemical demineralization process to effectively treat brine. Implementing the suggested process has the potential to improve the sustainability of the inland desalination by reducing the brine volume and its negative environmental impact.

## 1. Introduction

Freshwater scarcity has become a worldwide challenging issue.<sup>1-3</sup> To overcome freshwater scarcity in inland and semi-arid areas, including the Middle East, Southern California and Texas, reverse osmosis (RO) membrane desalination of brackish groundwater that contains total dissolved solids (TDS) ranging from 1 to 10 g/L is employed to generate freshwater.<sup>4-6</sup> Water recovery of brackish water RO desalination is typically between 40% and 85%, depending on TDS and chemical composition of the feed water.<sup>7-10</sup> Therefore, 15% to 60% of the feedwater becomes the RO concentrate waste, known as brine. However, the management of a RO concentrate stream remains challenging due to the high costs and adverse environmental impacts, especially in inland regions.<sup>11-13</sup> Current management options for inland desalination plants include ocean or surface water discharge through a brine line, deep well injection, evaporation pond, and landfill solidification.<sup>14-17</sup> However, the cost of existing brine management can add up to more than 30% of the overall treatment cost,<sup>18,19</sup> and direct disposal can have negative environmental impacts by increasing salinity and inducing secondary pollution.<sup>20-22</sup>

In order to minimize the inland brine management cost and negative environmental effects, additional water recovery from brine is needed. The improvement of water recovery can be achieved by passing the primary brine through a secondary RO process.<sup>23,24</sup> However, the major limitation to achieving high water recovery from the brine is mineral scaling by sparingly soluble salts (*e.g.*, calcite and gypsum) on the membrane surface.<sup>25,26</sup> Therefore, an adequate brine treatment prior to the further membrane process is necessary to reduce mineral scaling during the secondary RO process.

The major target constituents of brine pre-treatment are antiscalant and scale-forming precursors.<sup>17,27–29</sup> Antiscalant is a vital chemical due to its scale inhibition effect, which improves the water recovery of the RO system; therefore, the type of antiscalant applied to the RO system has a significant impact on the operating and maintenance costs in the desalination plants.<sup>30</sup> Choosing the appropriate type of antiscalants depends on the feedwater composition.<sup>31</sup> Among various types of antiscalants, phosphonate-based antiscalants are most commonly added to the feed water.<sup>32–34</sup> Although antiscalants help prevent precipitation and increase water recovery at the main RO desalination stage, the presence of antiscalants in the brine hinder the removal of target scale-forming precursors at the brine treatment process,<sup>35</sup> therefore, the removal of antiscalant can benefit brine treatment. Several antiscalant separation techniques, including use of coagulant or surfactant, ion exchange, adsorption, nanofiltration, and chemically-enhanced seeded precipitation have been proposed.<sup>29,36–42</sup> Additional chemical residuals may cause membrane fouling at the secondary RO process.<sup>43,44</sup> Ion exchange and adsorption still need to be improved for the process sustainability, and antiscalant residual may still present after treatment.

Antiscalant degradation by advanced oxidation processes (AOPs) is a promising approach to remove phosphonate-based antiscalant compounds.<sup>28,45–47</sup> The benefit of AOPs is the decomposition of antiscalants in brine to simple organic compounds. Consequently, both scale inhibition effect during the demineralization process and the possibility of membrane fouling by excessive antiscalant in the RO process can be reduced. Among various AOPs, an ultraviolet-driven persulfate oxidation process (UV/PS) has the potential to remove antiscalants effectively.<sup>46</sup> UV photolysis of persulfate ( $S_2O_8^{2-}$ ) generates sulfate radical ( $SO_4^{\bullet-}$ ), and it is a strong oxidant with similar oxidizing power ( $E^0 = 2.5 - 3.1$  V) to  $HO^{\bullet}$  ( $E^0 = 1.9 - 2.7$  V).  $SO_4^{\bullet-}$  is

also more selective toward organic contaminants.<sup>48</sup> However, little research has been performed on the application of UV/PS on brine treatment.

After antiscalant degradation, the removal of scale-forming precursors in brine can be achieved by demineralization processes. Among various demineralization techniques, chemical demineralization (CDM) is effective in the removal of scale-forming precursors.<sup>49–51</sup> Alkaline chemicals, *e.g.*, CaO, Ca(OH)<sub>2</sub>, NaOH, NaHCO<sub>3</sub>, Na<sub>2</sub>CO<sub>3</sub> are often used to remove major scale forming precursors including Ca<sup>2+</sup>, Ba<sup>2+</sup>, Mg<sup>2+</sup>, and SiO<sub>2</sub>.<sup>51–54</sup> NaOH softening and lime softening using CaO, Ca(OH)<sub>2</sub>, NaHCO<sub>3</sub> or Na<sub>2</sub>CO<sub>3</sub> would be beneficial, because these methods only require simple chemical addition; as a result, it allows for the recovery of relatively pure minerals from the sludge of the CDM process. Nonetheless, the kinetics and mechanisms of CDM after antiscalant degradation via UV/PS remains unknown, and the impact of UV/PS and CDM processes on system water recovery needs to be answered.

The objectives of this research were to: (1) evaluate the applicability of the UV/PS coupled with CDM to degrade antiscalant and remove scale-forming precursors from brackish water desalination brine; (2) determine operating conditions of the UV/PS process (*i.e.*, persulfate dose and UV irradiation time) to degrade antiscalant in the feed water; (3) identify the kinetics and mechanisms of calcium precipitation and calcium removal efficiency by NaOH softening and lime softening methods in the presence and absence of UV/PS pre-treatment at the CDM process; (4) investigate the solid/liquid separation performance of the MF process after CDM in the absence and presence of the UV/PS process, and (5) assess the water recovery potential at RO after UV/PS-CDM process. The performance of the UV/PS-CDM process was evaluated based on a few technical evaluation metrics, including the settling rate of mineral precipitates at the CDM process, product water quality, and the extent of MF membrane fouling.

## 2. Materials and Methods

### 2.1 Chemicals and solutions

Stock solutions and synthetic brine feed water were prepared using Milli-Q water. All chemicals are reagent grade or higher and obtained from JT Baker, Sigma-Aldrich, or Fisher Scientific. Synthetic brine solutions were prepared to simulate the chemical composition of inland brackish groundwater RO concentrate at the Inland Empire Brine Line in Riverside, California, USA.<sup>55</sup> Details of brine water quality are listed in Table 1. The use of synthetic feed water allowed a fundamental investigation of the calcium carbonate precipitation, which is a major supersaturated solid in inland desalination brines.<sup>41,56</sup> Diethylenetriamine pentamethylene phosphonic acid (DTPMP) was chosen as a representative phosphonate-based antiscalant to prepare the synthetic brine, because DTPMP is a widely used antiscalant in membrane treatment and exhibits a strong scaling inhibition effect.<sup>33,35</sup> The chemical structure of DTPMP is shown in Fig. S1.

### 2.2 Experimental setup

The brine treatment process consisted of a UV/PS pre-treatment to degrade antiscalant, a CDM step to remove scaling components, and a microfiltration (MF) step to separate scaling minerals from the treated brine (Fig. ). For UV/PS experiments, a 4-L beaker UV reactor equipped with a 450-W medium pressure UV immersion lamp (Ace Glass, Inc.) was utilized (Fig. S2A). To start an experiment, a 3.5-L synthetic brine solution containing 2-5 mM persulfate and 0.1 mM DTPMP (equivalent to 15.5 mg/L as organic phosphorus) was exposed to UV irradiation that last up to 60 minutes. The initial and final pH of the brine solutions was 7.8 and 6.7, respectively. The chosen concentration of DTPMP was at the higher end of typical phosphonate-based antiscalant concentration observed in RO brine.<sup>39,57</sup> During UV/PS experimentation, 3-mL samples were withdrawn by pipette from the experimental reservoirs at each targeted reaction

time interval. Additional details on the UV/PS experiment can be found in Text S1 of the Supplementary Information.

Following the UV/PS experiment, 1L of the UV/PS treated brine underwent a CDM process in a 2-L stirred rectangular batch reactor (Fig. S2B). For the UV/PS pre-treatment prior to the CDM process, 4 mM persulfate and 5, 10, or 20 minutes of UV irradiation time were employed. In addition, two control CDM experiments were conducted using a synthetic brine without UV/PS pre-treatment (control – no UV/PS pre-treatment), and a synthetic brine in the absence of antiscalant without UV/PS pre-treatment (control – no antiscalant). Two chemical demineralization methods were evaluated for the CDM process, *i.e.*, NaOH softening and lime softening. For the NaOH softening method, a targeted amount of NaOH was added to adjust the pH of the UV/PS-treated brine to either 7.8, 9.0 or 10.2 with prior to CDM process. pH 7.8 is synthetic RO brine feedwater pH (Table 1), pH 10.2 is where the plateau of the calcium carbonate saturation index in the brine started (Fig. S3), and pH 9 is the middle point of those two pHs. For the lime softening method, a requisite amount of  $\text{Ca}(\text{OH})_2$  and  $\text{NaHCO}_3$  in combination was added to the UV/PS-treated brine. Immediately after chemical addition, the brine was rapid-mixed at 700 rpm for 1 minute to allow chemical mixing, followed by 29 minutes of sedimentation (*i.e.*, a total of 30 mins of CDM process). At targeted time intervals during the CDM process, 3-mL samples were withdrawn from the batch reactor at 3 cm below the water-air interface using a pipette, which minimized the stirring impact on the reactor (Fig. S2B). All samples were immediately acidified with 100  $\mu\text{L}$  of concentrated  $\text{HNO}_3$  and preserved for total calcium analysis.

Following the CDM process, a MF step was conducted to evaluate the impact of the UV/PS-CDM treatment on the solid/liquid separation process from the treated brine. Specifically, the

CDM treated brine further underwent a dead-end microfiltration (MF) process to separate residual particles in the supernatant.<sup>58–61</sup> Based on the CDM process results, the solid/liquid separation was performed 3 minutes of the lime softening CDM process and 5 minutes after the start point of NaOH softening CDM process with different UV/PS pre-treated brines. The experimental setup consisted of 0.1- $\mu\text{m}$  polyvinylidene fluoride membrane (Millipore Sigma, Burlington, MA), pressurizing equipment (nitrogen gas tank, pressure gauge, and pressure control valve), a 200 mL stirred cell (Millipore Sigma, Burlington, MA), and a permeate collection line (Fig.S4 and Text S2). The permeate flux was measured continuously by a digital mass balance. Membrane permeate flux and relative permeate flux were calculated using Equations 1-2, respectively:

$$J = \frac{M}{At} \quad (\text{E1})$$

$$\text{Relative permeate flux} = \frac{J}{J_0} \quad (\text{E2})$$

Where  $J$  is the permeate flux ( $\text{g cm}^{-2} \text{s}^{-1}$ ),  $M$  is total mass of permeate (g),  $A$  is membrane area ( $\text{cm}^2$ ),  $t$  is experimental time (s), and  $J_0$  is initial permeate flux ( $\text{g cm}^{-2} \text{s}^{-1}$ ).

### 2.3 Analytical methods for water samples

During the UV/PS pre-treatment, the concentration of persulfate in the brine was determined by a colorimetric method using potassium iodide.<sup>62</sup> The concentration of DTPMP in the brine was calculated by measuring orthophosphate concentration using Standard method 4500-P E,<sup>63</sup> since orthophosphate is the final phosphorus oxidation product.<sup>46,58</sup> During the CDM experimental step, the solid precipitation and sedimentation were monitored by measuring the change of total calcium concentration at pre-determined time intervals. The concentrations of total calcium and sodium in the initial synthetic brine and sampled product solutions were determined using an

Inductively Coupled Plasma Mass Spectroscopy (ICP-MS, Agilent Technologies, Palo Alto, CA). Alkalinity was measured by titration based on standard method 2320B and the concentration of chloride was determined following Standard Methods 4110B by ion chromatography (Dionex ICS-1100, Thermo Scientific, Sunnyvale, CA).<sup>63</sup>

### 3. Results and discussion

#### 3.1 Antiscalant DTPMP degradation by UV/persulfate

DTPMP was successfully degraded in synthetic brine as the brine was irradiated in the UV/persulfate system (Fig. 2. Contribution of persulfate dose to DTPMP degradation (A) effect of UV/persulfate on DTPMP degradation and (B) observed *pseudo* first-order rates of DTPMP degradation. Experimental condition: Synthetic brine, [Ionic strength] = 98 mM; [DTPMP]<sub>0</sub> = 0.1 mM; [Persulfate]<sub>0</sub> = 2.0 - 5.0 mM; initial pH = 7.8; Error bars represent the range of values for triplicate tests.A). The degradation of DTPMP followed a *pseudo* first-order kinetics model (all R<sup>2</sup> > 0.95). The observed *pseudo* first-order rates of DTPMP degradation increased from 5.9×10<sup>-2</sup> to 9.6×10<sup>-2</sup> min<sup>-1</sup> as the persulfate dosage increased from 2 to 5 mM (Fig. 2. Contribution of persulfate dose to DTPMP degradation (A) effect of UV/persulfate on DTPMP degradation and (B) observed *pseudo* first-order rates of DTPMP degradation. Experimental condition: Synthetic brine, [Ionic strength] = 98 mM; [DTPMP]<sub>0</sub> = 0.1 mM; [Persulfate]<sub>0</sub> = 2.0 - 5.0 mM; initial pH = 7.8; Error bars represent the range of values for triplicate tests.B).

Persulfate photolysis generates SO<sub>4</sub><sup>•-</sup> (Reaction 1), which further hydrolyzes to HO<sup>•</sup> (Reaction 2; k<sub>2</sub>=6.5×10<sup>7</sup> M<sup>-1</sup>s<sup>-1</sup>):<sup>64,65</sup>





A persulfate dosage equal or higher than 4 mM completely degraded DTPMP in 30 minutes UV irradiation time; however, a persulfate dosage less than 4 mM were not enough to completely degrade 0.1 mM DTPMP (Fig. 2A), due to an insufficient generation of reactive radicals via persulfate photolysis (R1 - R2).

$\text{SO}_4^{\bullet-}$  and  $\text{HO}^\bullet$  can be scavenged by persulfate (Reactions 3-4;  $k_3=5.5 \times 10^5 \text{ M}^{-1}\text{s}^{-1}$ ;  $k_4=1.4 \times 10^7 \text{ M}^{-1}\text{s}^{-1}$ ), respectively,<sup>46,66</sup> and generate non-reactive persulfate radical  $\text{S}_2\text{O}_8^{\bullet-}$ :<sup>67,68</sup>



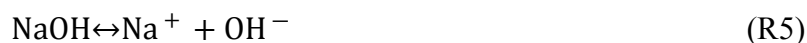
This scavenging impeded the degradation of DTPMP with increasing persulfate dosage; therefore, the rate constant of DTPMP degradation increased at a slower pace as the persulfate dosage increased beyond 4 mM (Fig. 2B). Because more than 90% of DTPMP was degraded after 20 minutes of persulfate photolysis with 4 mM persulfate dosage (Fig. 2. Contribution of persulfate dose to DTPMP degradation (A) effect of UV/persulfate on DTPMP degradation and (B) observed *pseudo* first-order rates of DTPMP degradation. Experimental condition: Synthetic brine, [Ionic strength] = 98 mM; [DTPMP]<sub>0</sub> = 0.1 mM; [Persulfate]<sub>0</sub> = 2.0 - 5.0 mM; initial pH = 7.8; Error bars represent the range of values for triplicate tests.B), 4 mM dosage of persulfate was chosen for subsequent UV/PS-CDM experiments.

### 3.2 Chemical demineralization by NaOH Softening

Calcium carbonate is a major precipitate from the brine, and the precipitation of calcium carbonate is dictated by pH of the solution as a result of carbonate speciation.<sup>69</sup> The saturation index (SI, the logarithm value of the saturation state) of calcium carbonate of the brine was

approximately 1.8 (Fig. S3), indicating precipitation is thermodynamically favorable ( $SI > 0$ ).

When NaOH is added to the brine to increase pH, chemical demineralization occurs via calcium carbonate precipitation (Reactions 5-7):

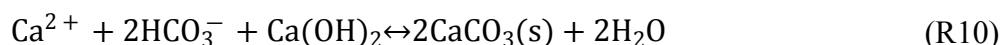
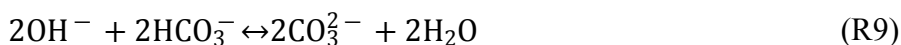
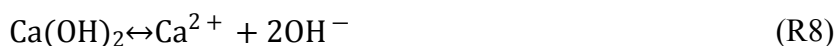


Therefore, the saturation index of calcium carbonate mineral increases as pH increases (Fig. S3). Experimental data showed that total calcium residual in the brine exhibited the biggest decrease when the brine pH was adjusted to 10.2 during the CDM process (Fig. 3A). When the brine pH increased from pH 7.8 to pH 10.2, the dominant carbonate species switches from  $\text{HCO}_3^-$  to  $\text{CO}_3^{2-}$  and promoted calcium precipitation (R5 - R7).

In comparison with the control without UV/PS pre-treatment, the UV/PS pre-treatment was shortening the settling time of calcium precipitates during the CDM process and achieved the lowest final calcium concentration (Fig. 3B). In addition, the total calcium removal from the UV/PS pre-treated brine during the CDM process exhibited a similar reaction kinetics in comparison to the CDM control without antiscalant (Fig. 3B). These trends strongly suggested that the degradation of DTPMP during the UV/PS pre-treatment promoted calcium removal during the CDM process. The presence of DTPMP has a detrimental effect on the calcium removal and delayed the sedimentation of calcium precipitates during the CDM (Control without UV/PS pre-treatment in Fig. 3A). Antiscalants interfere with the complete particle growth by adsorbing onto nucleating crystals and blocking the crystal growth sites.<sup>70,71</sup>

### 3.3 Chemical demineralization by lime softening

Chemical demineralization via lime softening introduces additional calcium in the form of hydrated lime  $\text{Ca}(\text{OH})_2$  into the system and induces calcium carbonate precipitation (Reactions 8-10):



Since additional calcium was added for demineralization, total calcium concentration increased initially during the first one minute and then decreased as reactions took place (Fig. ). During the lime softening CDM process, total calcium concentration in the UV/PS pre-treated brine exhibited the fastest removal in comparison to controls (Fig. 4). The settling of calcium precipitates mostly took place during the first 3 minutes of the CDM process. In contrast, no calcium removal was achieved after 15 minutes of CDM process in the two control experiments.

In addition, as DTPMP was degraded to orthophosphate during the UV/PS pre-treatment, the formation of orthophosphate accelerated total calcium removal during the CDM process. In a separate control experiment by adding orthophosphate to the brine prior to the CDM process, the effects of orthophosphate addition on the kinetics of total calcium removal were similar to UV/PS pre-treatment. This behavior was observed for both NaOH softening (Fig. S5A) and lime softening (Fig. S5B). The formation of orthophosphate resulted in the supersaturation and precipitation of hydroxyapatite  $\text{Ca}_5(\text{PO}_4)_3\text{OH}_{(\text{s})}$  in the brine (saturation index > 14.4), which could accelerate the nucleation and precipitation of calcium solids. Therefore, the UV/PS pre-treatment both removed the inhibitive effect of DTPMP on calcium precipitation and accelerated

additional calcium phosphate mineral nucleation, both of which contributed to the total calcium removal during the CDM process.

The effect of varying UV irradiation time during the UV/PS pre-treatment on total calcium removal via the CDM process was also investigated. Results showed that an increased in the UV irradiation time led to better total calcium removal during the NaOH softening CDM process (Fig. 5A). For the lime softening CDM process, notably a faster settling was achieved with UV/PS pre-treatment regardless of the UV irradiation time (Fig. 5B), indicating that a partial degradation of DTPMP also accelerated the demineralization process.

### **3.4 Microfiltration performance following chemical demineralization**

The CDM-treated brine further underwent a MF process and the effect of UV/PS pre-treatment on the MF performance was evaluated. Results showed that the MF permeate flux maintained at a high level and exhibited little decline when the brine was pre-treated with the UV/PS as the first step (Fig. ). This trend suggested that the UV/PS pre-treatment significantly alleviated particle scaling on the MF membrane surface. Because the UV/PS pre-treated brine exhibited a fast settling of calcium solids and a majority of the solids were removed during the first 5 minutes of the CDM process, the combined UV/PS-CDM treated brine feeding into the MF step had minimal suspended solids. Consequently, the MF permeate fluxes showed a minimal decline. In contrast, the brine without UV/PS pre-treatment exhibited a severe flux decline (50% -80% decrease) during the MF separation (Fig. ). Without antiscalant degradation by the UV/PS pre-treatment, a significant amount of precipitates remained after the CDM process in the solution due to slow settling rate, which induced fouling on the MF membrane by precipitates and promotes a denser fouling cake.<sup>35</sup> The less fouling on the MF membrane indicates that

increase in product water yield, less frequent membrane backwashing and replacement, and reduced MF operation cost.

#### 4. Engineering Implications on Freshwater Recovery

The application of the UV/PS pre-treatment followed by a CDM process improves the permeate flux during the MF step due to a low calcium concentration in the MF permeate (Table S1). The MF permeate can further undergo an additional RO step to recover freshwater from the sequential UV/PS-CDM-MF treated brine. The extent of water recovery via this additional RO step is limited by calcite mineral scaling on the RO membrane, which can be predicted based on the theoretical calculations on the saturation index (SI) of calcite in the UV/PS-CDM-MF treated brine (*i.e.*, RO feed brine). Details on the SI calculations are provided in Text S3 and Table S1. Calcite is oversaturated in the untreated brackish desalination brine and its oversaturation leads to membrane scaling during the RO step and limits water recovery. Specifically, water recovery can be continuously achieved via the additional RO system in the absence of antiscalant when the calcite SI of the feed brine is below zero, *i.e.*, the sequential UV/PS-CDM-MF treated brine is undersaturated with respect to calcite. Furthermore, additional antiscalant can be added to the UV/PS-CDM-MF treated brine to alleviate calcite scaling. For a conservative RO system design, the upper operating limit of calcite SI is recommend to be 1.8 for the RO feed water with phosphonate-based antiscalants to avoid extreme operating condition or system failure.<sup>72</sup>

Calculations show that the calcite SI of the untreated brine (control without treatment), UV/PS-CDM-MF treated brine (via lime softening during the CDM process) and UV/PS-CDM-MF treated brine (via NaOH softening during the CDM process) was 1.8, 0.3 and -0.2, respectively (Fig. ). This suggests that that the untreated brine is an unfavorable condition for additional water

recovery. When an antiscalant is added during the additional RO step to recover freshwater from the treated brine, the NaOH softening based UV/PS-CDM-MF treatment train can achieve more than 90% freshwater recovery until the SI limit (*i.e.*, a value of 1.8) of antiscalant inhibition is reached (Fig. ). Similarly, the lime softening based UV/PS-CDM-MF treatment train can achieve more than 85% freshwater recovery until the SI limit is reached (Fig. ).

## 5. Conclusions

The performance of the sequential UV/PS-CDM-MF treatment train process was evaluated and compared to control experiments. The results show that the UV/PS-CDM-MF in combination is a promising inland desalination brine treatment technology to remove oversaturated calcium and increase the freshwater recovery potential via an additional RO step. UV/persulfate process effectively degraded phosphonate-based antiscalant. In addition, the CDM process after UV/PS pre-treatment achieved faster settling rate of calcium precipitates due to antiscalant degradation by the UV/PS pre-treatment. Both NaOH- and lime-softening based CDM methods prevent flux decline during the subsequent microfiltration step and extend the duration of operation during the calcium solid/treated brine separation process. The application of the UV/PS-CDM-MF treatment train process has the potential to remove more than 90% calcium from inland desalination brine. As a result, a very high-water recovery (>90%) by an additional RO process is expected. Future work will evaluate the applicability of the UV/PS-CDM-MF-RO treatment train for freshwater recovery and hardness mineral recoveries from inland desalination brine.

## Acknowledgement

This work was supported by funds from the United States Bureau of Reclamation (DWPR-R19AC00092) and an INTERN supplement to a U.S. National Science Foundation Career

Award (CBET-1653931). The authors thank Carlos Quintero and Richard Haller at Santa Ana Watershed Project Authority for assistance in sample collection and discussion.

Table 1. Chemical composition of brackish water desalination brine solutions.

<b>Parameter</b>	<b>Synthetic Brine water quality in this study</b>	<b>Brine water quality of Inland Empire Brine Line</b>	<b>Unit</b>
<b>Total Dissolved Solids</b>	5900	5100	mg/L
<b>Calcium</b>	660	660	mg/L
<b>Sodium</b>	1260	800	mg/L
<b>Bicarbonate</b>	1300	1300	mg/L
<b>Chloride</b>	2200	2200	mg/L
<b>Antiscalant</b>	15.5	1	mg P/L
<b>pH</b>	7.8	7.8	--
<b>Ionic strength</b>	98*	98	mM
<b>Calcite Saturation Index</b>	1.8	1.8	--
<b>Temperature</b>	23	23	°C

\*NaClO<sub>4</sub> was added to the synthetic brine to reach the targeted ionic strength value.

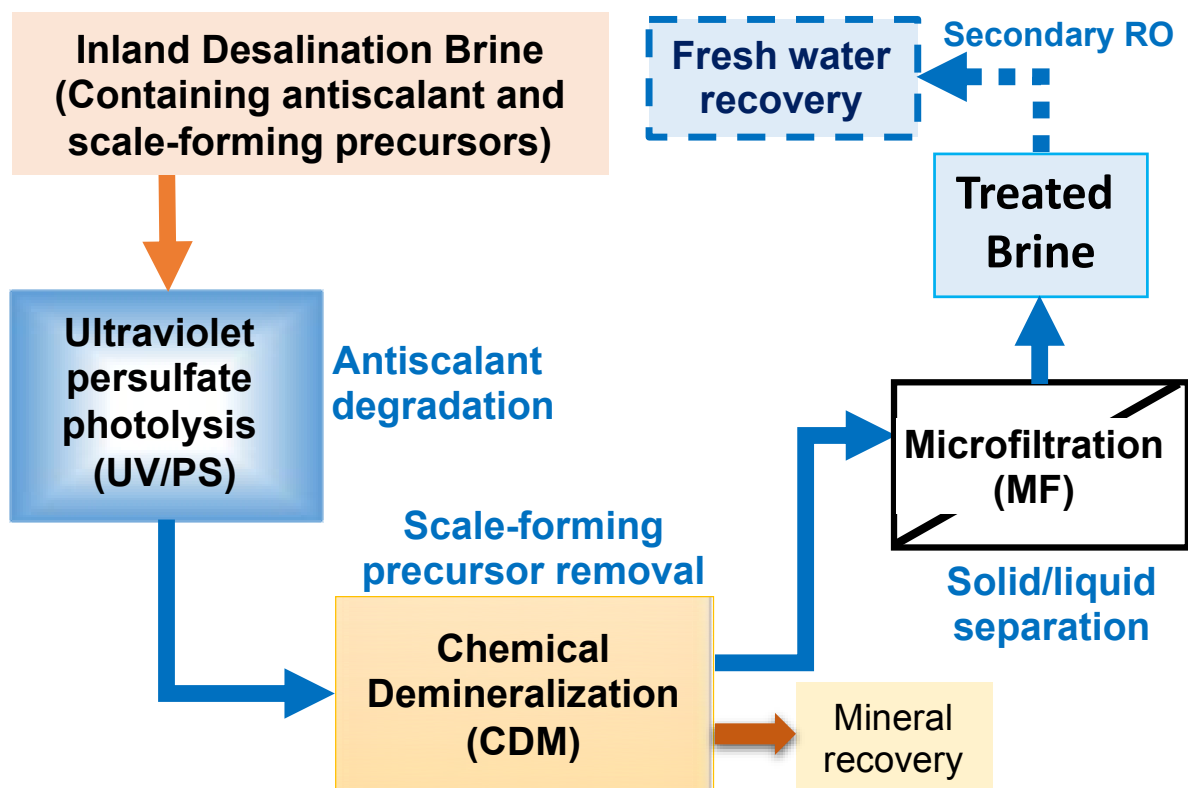


Fig. 1. A schematic of the UV/PS-CDM-MF brine pre-treatment developed in this study.

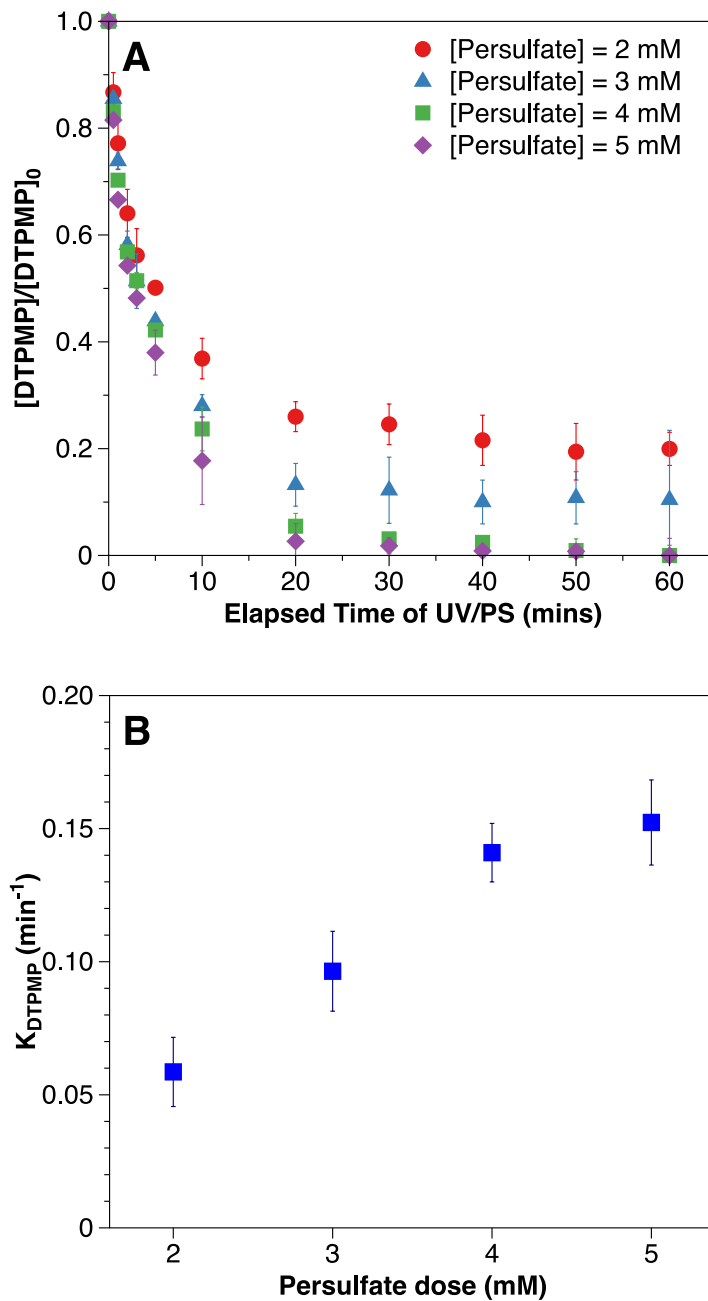


Fig. 2. Contribution of persulfate dose to DTPMP degradation (A) effect of UV/persulfate on DTPMP degradation and (B) observed *pseudo* first-order rates of DTPMP degradation.

Experimental condition: Synthetic brine, [Ionic strength] = 98 mM; [DTPMP]<sub>0</sub> = 0.1 mM; [Persulfate]<sub>0</sub> = 2.0 - 5.0 mM; initial pH = 7.8; Error bars represent the range of values for triplicate tests.

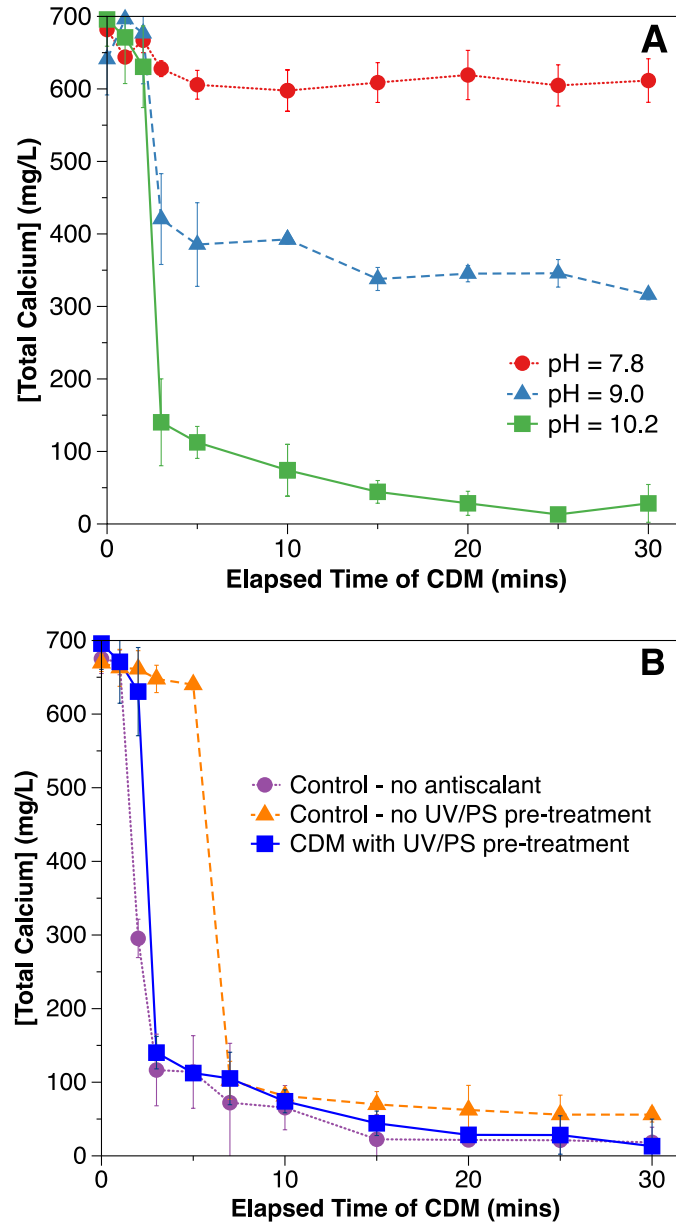


Fig. 3. Total calcium concentration of CDM process by NaOH softening with 5 M NaOH. (A) the CDM process with UV/PS pre-treatment at pH 7.8, pH 9, and pH 10.2; (B) The CDM process for controls and CDM process with UV/PS pre-treatment at pH 10.2. Note: after chemical addition (time zero), each solution was rapid-mixed at 700 rpm for 1 minute to allow chemical mixing and precipitation to occur and then sit for 29 mins for sedimentation (that is, a total elapsed time of 30 mins); Error bars represent the range of values for triplicate tests.

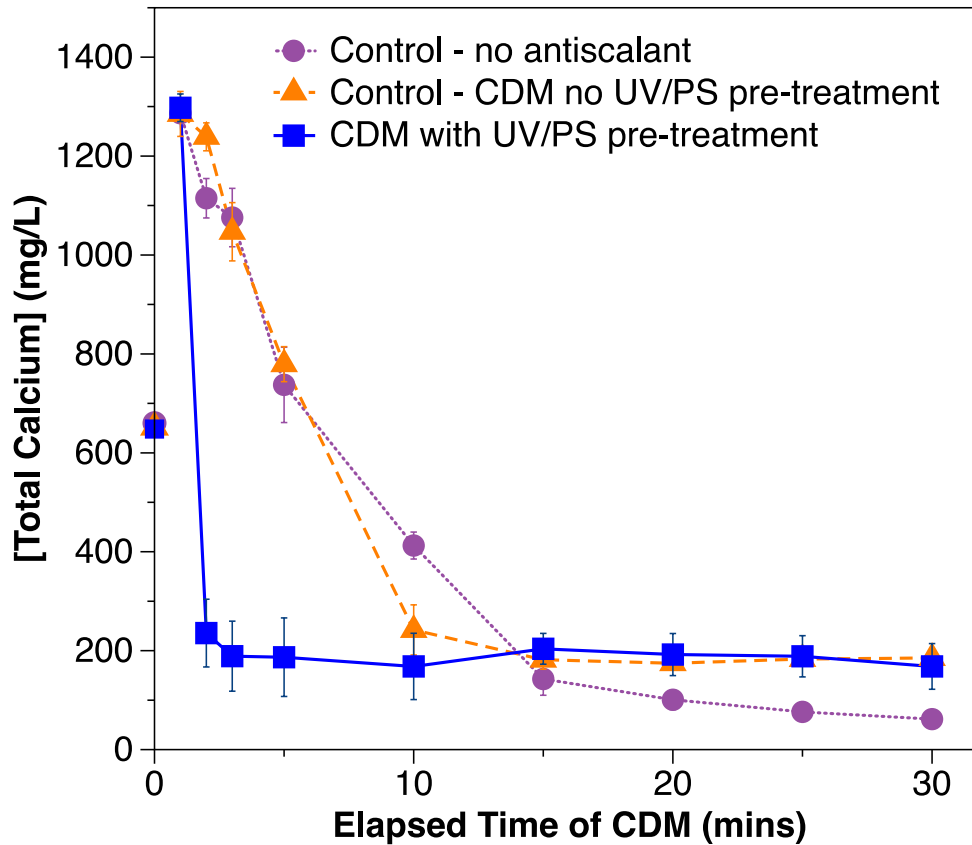


Fig. 4. Total calcium concentration of the CDM process by lime softening (16.5 mM of  $\text{Ca}(\text{OH})_2$  and 11.7 mM of  $\text{NaHCO}_3$ ). Note: after chemical addition (time zero), each solution was rapid-mixed at 700 rpm for 1 minute to allow chemical mixing and precipitation to occur and then sit for 29 mins for sedimentation (that is, a total elapsed time of 30 mins); Error bars represent the range of values for triplicate tests.

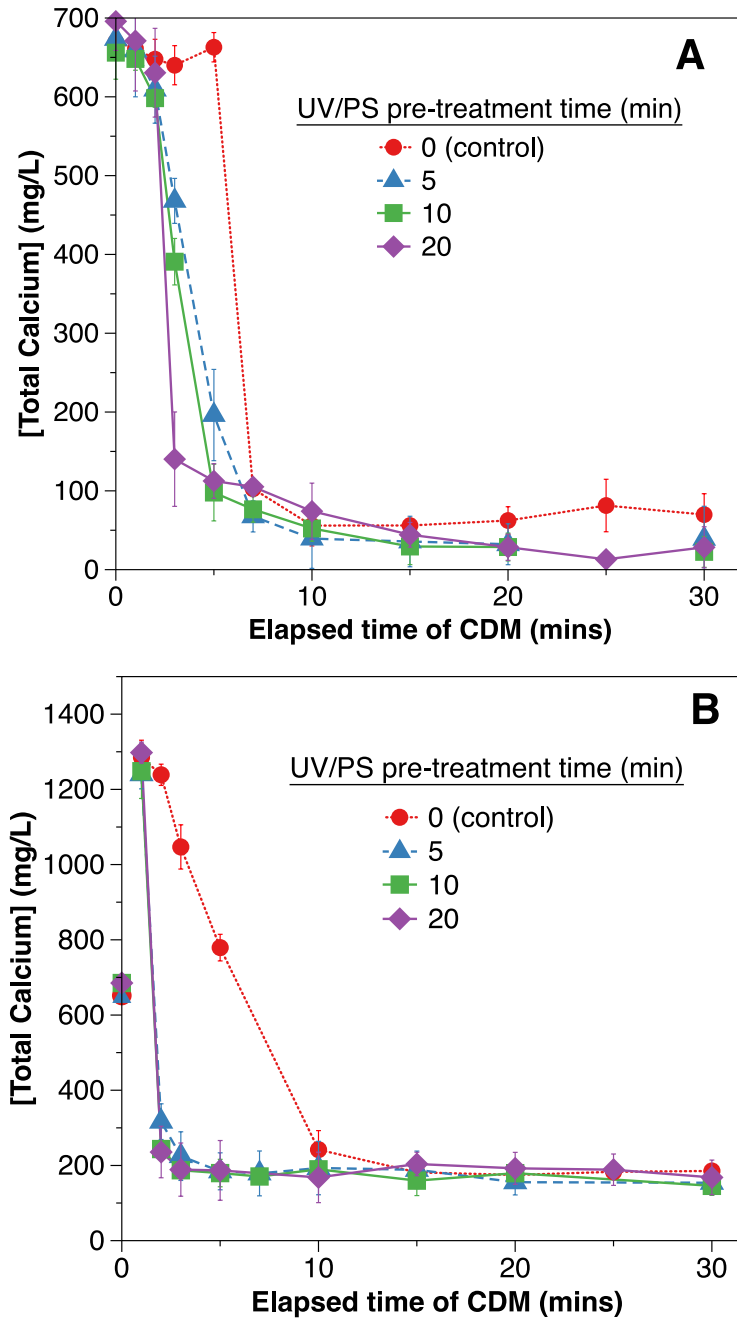


Fig. 5. Total calcium concentration change during the CDM process after 0, 5, 10, and 20 minutes UV/PS pre-treatment, (A) NaOH softening at pH 10.2; (B) lime softening (16.5 mM of Ca(OH)<sub>2</sub> and 11.7 mM of NaHCO<sub>3</sub>). Note: after chemical addition (time zero), each solution was rapid-mixed at 700 rpm for 1 minute to allow chemical mixing and precipitation to occur and then sit for 29 mins for sedimentation (Total 30 mins); Error bars represent the range of values for triplicate tests.

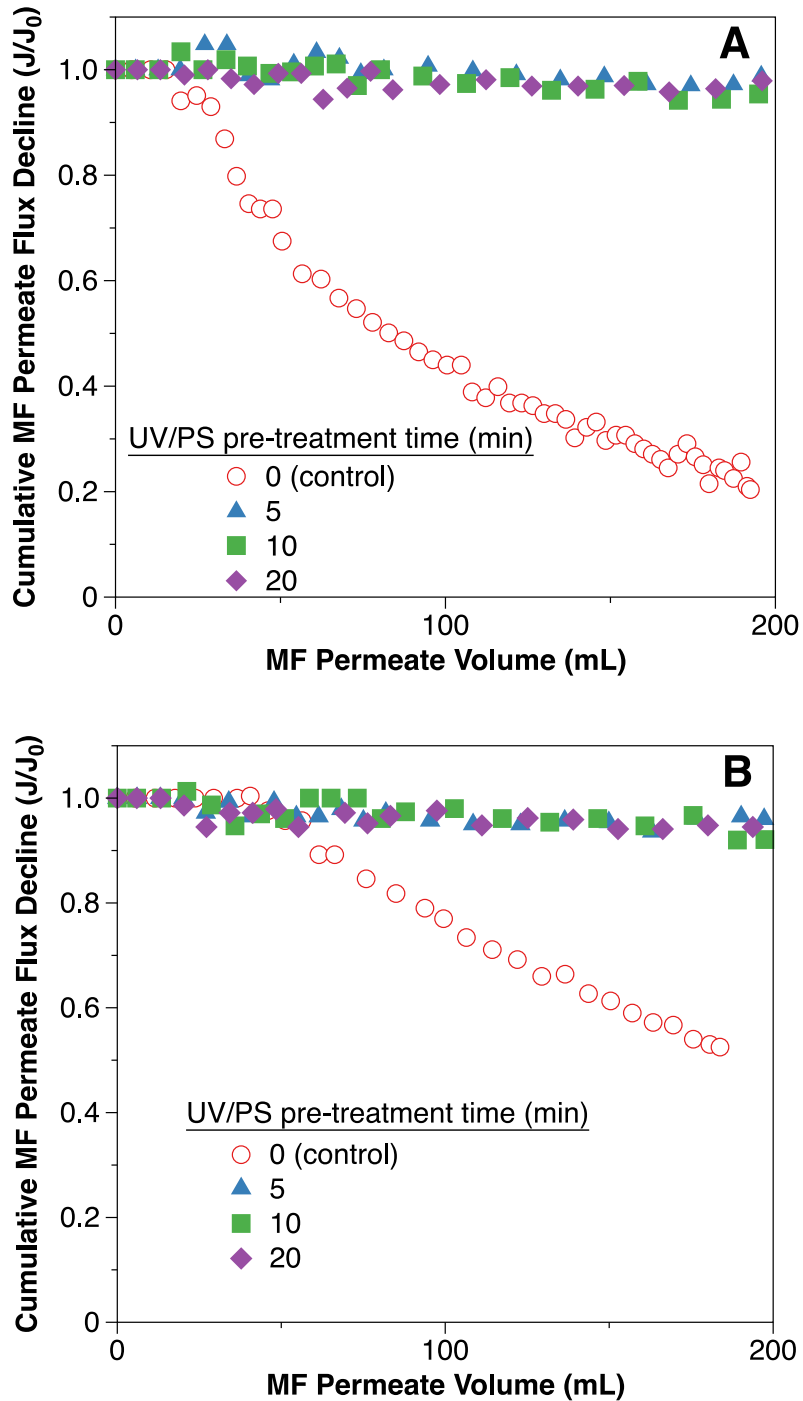


Fig. 6. Normalized permeate flux decline as a function of cumulative normalized volume throughput in the solutions of (A) NaOH softening (5 M NaOH, pH 10.2) and (B) lime softening demineralization without and with UV/PS pre-treatment.

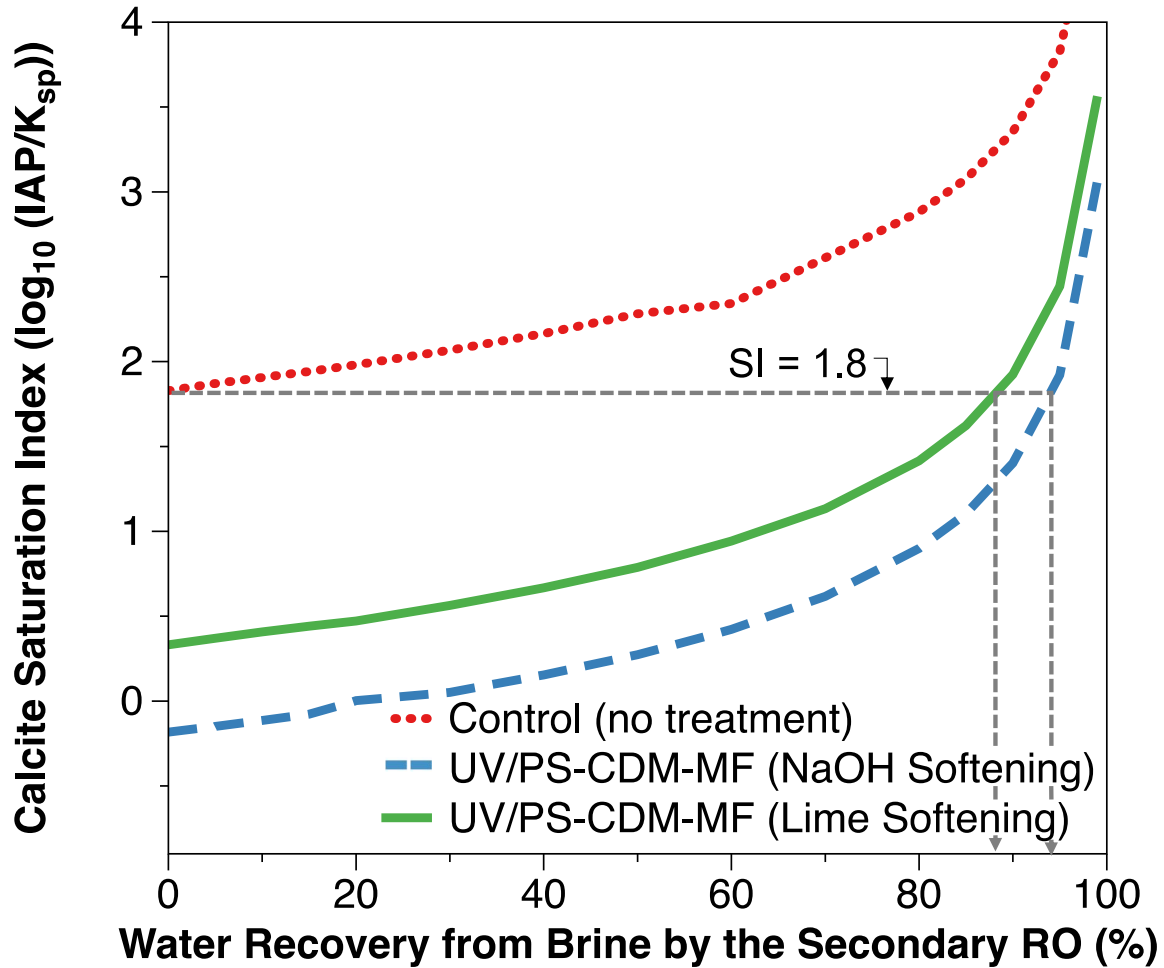


Fig. 7. Calcite saturation index calculations for calcite in the treated brine after UV/PS-CDM (NaOH softening) and UV/PS-CDM (lime softening). Control stands for no UV/PS-CDM treatment (direct use of brine). Saturation index calculations were performed through Visual Minteq (Version 3.1) for a pH of 7.8 with 100% salts rejection rate at the additional RO process, and input water quality parameters are in Table S1. Note: the ordinate is a saturation index, and it is a logarithmic number.

**REFERENCES**

- 1 M. M. Mekonnen and A. Y. Hoekstra, Sustainability: Four billion people facing severe water scarcity, *Sci. Adv.*, 2016, **2**, 1–7.
- 2 K. Schwabe, M. Nemat, C. Landry and G. Zimmerman, Water markets in the Western United States: Trends and opportunities, *Water (Switzerland)*, 2020, **12**, 1–15.
- 3 J. H. Yoon, S. Y. S. Wang, R. R. Gillies, B. Kravitz, L. Hipps and P. J. Rasch, Increasing water cycle extremes in California and in relation to ENSO cycle under global warming, *Nat. Commun.*, 2015, **6**, 8657.
- 4 N. K. Khanzada, S. J. Khan and P. A. Davies, Performance evaluation of reverse osmosis (RO) pre-treatment technologies for in-land brackish water treatment, *Desalination*, 2017, **406**, 44–50.
- 5 L. F. Greenlee, D. F. Lawler, B. D. Freeman, B. Marrot and P. Moulin, Reverse osmosis desalination: Water sources, technology, and today's challenges, *Water Res.*, 2009, **43**, 2317–2348.
- 6 M. R. Landsman, R. Sujani, S. H. Brodfuehrer, C. M. Cooper, A. G. Darr, R. J. Davis, K. Kim, S. Kum, L. K. Nalley, S. M. Nomaan, C. P. Oden, A. Paspureddi, K. K. Reimund, L. S. R. III, S. Yeo, D. F. Lawler, B. D. Freeman and L. E. Katz, Water Treatment: Are Membranes the Panacea?, *Annu. Rev. Chem. Biomol. Eng.*, 2020, **11**, 559–585.
- 7 B. C. McCool, A. Rahardianto, J. I. Faria and Y. Cohen, Evaluation of chemically-enhanced seeded precipitation of RO concentrate for high recovery desalting of high salinity brackish water, *Desalination*, 2013, **317**, 116–126.
- 8 M. Mickley, *Updated and Extended Survey of U.S. Municipal Desalination Plants*, 2018.
- 9 A. Almulla, M. Eid, P. Côté and J. Coburn, Developments in high recovery brackish water

- desalination plants as part of the solution to water quantity problems, *Desalination*, 2003, **153**, 237–243.
- 10 P. Malmrose, J. Lozier, M. Mickley, R. Reiss, J. Russell, J. Schaefer, S. Sethi, J. Manuszak, R. Bergman and K. Z. Atasi, *Committee report: Current perspectives on residuals management for desalting membranes*, 2004, vol. 96.
- 11 National Research Council, *Desalination: A national perspective*, National Academies Press, Washington, DC, 2008.
- 12 J. Morillo, J. Usero, D. Rosado, H. El Bakouri, A. Riaza and F. J. Bernaola, Comparative study of brine management technologies for desalination plants, *Desalination*, 2014, **336**, 32–49.
- 13 P. Bond and S. Veerapaneni, Zeroing in on ZLD technologies for inland desalination, *J. Am. Water Works Assoc.*, 2008, **100**, 76–89.
- 14 M. Ahmed, W. H. Shayya, D. Hoey and J. Al-Handaly, Brine Disposal from Inland Desalination Plants, *Water Int.*, 2002, **27**, 194–201.
- 15 V. B. Jensen and J. L. Darby, Brine disposal options for small systems in California's Central Valley, *J. Am. Water Works Assoc.*, 2016, **108**, 276–289.
- 16 U.S. Department of the Interior Bureau of Reclamation, *Brine-Concentrate Treatment and Disposal Options Report*, 2009.
- 17 X. Tang, S. Kum and H. Liu, Inland Desalination Brine Disposal : A Baseline Study from Southern California on Brine Transport Infrastructure and Treatment Potential, *ACS ES&T Eng.*, 2022, **2**, 456–464.
- 18 M. Ahmed, W. H. Shayya, D. Hoey and J. Al-Handaly, Brine disposal from reverse osmosis desalination plants in Oman and the United Arab Emirates, *Desalination*, 2001,

- 133**, 135–147.
- 19 I. Leitner and Associates, *Survey of U.S. Costs and Water Rates for Desalination and Membrane Softening Plants*, Denver, CO, 1997.
  - 20 P. Xu, T. Y. Cath, A. P. Robertson, M. Reinhard, J. O. Leckie and J. E. Drewes, Critical review of desalination concentrate management, treatment and beneficial use, *Environ. Eng. Sci.*, 2013, **30**, 502–514.
  - 21 T. Mezher, H. Fath, Z. Abbas and A. Khaled, Techno-economic assessment and environmental impacts of desalination technologies, *Desalination*, 2011, **266**, 263–273.
  - 22 B. K. Pramanik, L. Shu and V. Jegatheesan, A review of the management and treatment of brine solutions, *Environ. Sci. Water Res. Technol.*, 2017, **3**, 625–658.
  - 23 A. Malek, M. N. A. Hawlader and J. C. Ho, Design and economics of RO seawater desalination, *Desalination*, 1996, **105**, 245–261.
  - 24 M. A. Alghoul, P. Poovanaesvaran, K. Sopian and M. Y. Sulaiman, Review of brackish water reverse osmosis (BWRO) system designs, *Renew. Sustain. Energy Rev.*, 2009, **13**, 2661–2667.
  - 25 Q. Liu, G.-R. Xu and R. Das, Inorganic scaling in reverse osmosis (RO) desalination: Mechanisms, monitoring, and inhibition strategies, *Desalination*, 2019, **468**, 114065.
  - 26 E. Lyster, M. man Kim, J. Au and Y. Cohen, A method for evaluating antiscalant retardation of crystal nucleation and growth on RO membranes, *J. Memb. Sci.*, 2010, **364**, 122–131.
  - 27 A. Subramani, E. Cryer, L. Liu, S. Lehman, R. Y. Ning and J. G. Jacangelo, Impact of intermediate concentrate softening on feed water recovery of reverse osmosis process during treatment of mining contaminated groundwater, *Sep. Purif. Technol.*, 2012, **88**,

- 138–145.
- 28 L. F. Greenlee, B. D. Freeman and D. F. Lawler, Ozonation of phosphonate antiscalants used for reverse osmosis desalination: Parameter effects on the extent of oxidation, *Chem. Eng. J.*, 2014, **244**, 505–513.
- 29 B. C. McCool, A. Rahardianto and Y. Cohen, Antiscalant removal in accelerated desupersaturation of RO concentrate via chemically-enhanced seeded precipitation (CESP), *Water Res.*, 2012, **46**, 4261–4271.
- 30 A. Ruiz-García, I. Nuez, M. D. Carrascosa-Chisvert and J. J. Santana, Simulations of BWRO systems under different feedwater characteristics. Analysis of operation windows and optimal operating points, *Desalination*, 2020, **491**, 114582.
- 31 A. Ruiz-García and J. Feo-García, Antiscalant cost and maximum water recovery in reverse osmosis for different inorganic composition of groundwater, *Desalin. Water Treat.*, 2017, **73**, 46–53.
- 32 D. Hasson, A. Drak and R. Semiat, Induction times induced in an RO system by antiscalants delaying CaSO<sub>4</sub> precipitation, *Desalination*, 2003, **157**, 193–207.
- 33 T. Jain, E. Sanchez, E. Owens-Bennett, R. Trussell, S. Walker and H. Liu, Impacts of antiscalants on the formation of calcium solids: Implication on scaling potential of desalination concentrate, *Environ. Sci. Water Res. Technol.*, 2019, **5**, 1285–1294.
- 34 W. Yu, D. Song, W. Chen and H. Yang, Antiscalants in RO membrane scaling control, *Water Res.*, 2020, **183**, 115985.
- 35 L. F. Greenlee, F. Testa, D. F. Lawler, B. D. Freeman and P. Moulin, The effect of antiscalant addition on calcium carbonate precipitation for a simplified synthetic brackish water reverse osmosis concentrate, *Water Res.*, 2010, **44**, 2957–2969.

- 36 T. Istirokhatun, M. N. Dewi, H. I. Ilma and H. Susanto, Separation of antiscalants from reverse osmosis concentrates using nanofiltration, *Desalination*, 2018, **429**, 105–110.
- 37 L. Boels, T. Tervahauta and G. J. Witkamp, Adsorptive removal of nitrilotris(methylenephosphonic acid) antiscalant from membrane concentrates by iron-coated waste filtration sand, *J. Hazard. Mater.*, 2010, **182**, 855–862.
- 38 L. Boels, K. J. Keesman and G. J. Witkamp, Adsorption of phosphonate antiscalant from reverse osmosis membrane concentrate onto granular ferric hydroxide, *Environ. Sci. Technol.*, 2012, **46**, 9638–9645.
- 39 Y. Chen, J. C. Baygents and J. Farrell, Removing phosphonate antiscalants from membrane concentrate solutions using granular ferric hydroxide, *J. Water Process Eng.*, 2017, **19**, 18–25.
- 40 S. E. H. Comstock, T. H. Boyer and K. C. Graf, Treatment of nanofiltration and reverse osmosis concentrates: Comparison of precipitative softening, coagulation, and anion exchange, *Water Res.*, 2011, **45**, 4855–4865.
- 41 M. Azadi Aghdam, F. Zraick, J. Simon, J. Farrell and S. A. Snyder, A novel brine precipitation process for higher water recovery, *Desalination*, 2016, **385**, 69–74.
- 42 Q. Yang, D. Lisitsin, Y. Liu, H. David and R. Semiat, Desupersaturation of RO concentrates by addition of coagulant and surfactant, *J. Chem. Eng. Japan*, 2007, **40**, 730–735.
- 43 M. M. Kim, J. Au, A. Rahardianto, J. Glater, Y. Cohen, F. W. Geringer and C. J. Gabelich, Impact of conventional water treatment coagulants on mineral scaling in RO desalting of brackish water, *Ind. Eng. Chem. Res.*, 2009, **48**, 3126–3135.
- 44 C. Baudequin, Z. Mai, M. Rakib, I. Deguerry, R. Severac, M. Pabon and E. Couallier,

- Removal of fluorinated surfactants by reverse osmosis - Role of surfactants in membrane fouling, *J. Memb. Sci.*, 2014, **458**, 111–119.
- 45 E. Rott, R. Minke, U. Bali and H. Steinmetz, Removal of phosphonates from industrial wastewater with UV/FeII, Fenton and UV/Fenton treatment, *Water Res.*, 2017, **122**, 345–354.
- 46 Z. Wang, G. Chen, S. Patton, C. Ren, J. Liu and H. Liu, Degradation of nitrilotris-methylenephosphonic acid (NTMP) antiscalant via persulfate photolysis: Implications on desalination concentrate treatment, *Water Res.*, 2019, **159**, 30–37.
- 47 Z. Bin Xu, W. L. Wang, N. Huang, Q. Y. Wu, M. Y. Lee and H. Y. Hu, 2-Phosphonobutane-1,2,4-tricarboxylic acid (PBTCA) degradation by ozonation: Kinetics, phosphorus transformation, anti-precipitation property changes and phosphorus removal, *Water Res.*, 2019, **148**, 334–343.
- 48 W. Li, S. Patton, J. M. Gleason, S. P. Mezyk, K. P. Ishida and H. Liu, UV Photolysis of Chloramine and Persulfate for 1,4-Dioxane Removal in Reverse-Osmosis Permeate for Potable Water Reuse, *Environ. Sci. Technol.*, 2018, **52**, 6417–6425.
- 49 J. Rioyo, V. Aravinthan, J. Bundschuh and M. Lynch, Research on ‘high-pH precipitation treatment’ for RO concentrate minimization and salt recovery in a municipal groundwater desalination facility, *Desalination*, 2018, **439**, 168–178.
- 50 A. Rahardianto, B. C. McCool and Y. Cohen, Accelerated desupersaturation of reverse osmosis concentrate by chemically-enhanced seeded precipitation, *Desalination*, 2010, **264**, 256–267.
- 51 C. J. Gabelich, M. D. Williams, A. Rahardianto, J. C. Franklin and Y. Cohen, High-recovery reverse osmosis desalination using intermediate chemical demineralization, *J.*

- Memb. Sci.*, 2007, **301**, 131–141.
- 52 Z. Wang, P. Sun, Y. Li, T. Meng, Z. Li, X. Zhang, R. Zhang, H. Jia and H. Yao, SI: Reactive Nitrogen Species Mediated Degradation of Estrogenic Disrupting Chemicals by Biochar/Monochloramine in Buffered Water and Synthetic Hydrolyzed Urine, *Environ. Sci. Technol.*, 2019, **53**, 12688–12696.
- 53 Y. Yin, W. Wang, A. K. Kota, S. Zhao and T. Tong, Elucidating mechanisms of silica scaling in membrane distillation: Effects of membrane surface wettability, *Environ. Sci. Water Res. Technol.*, 2019, **5**, 2004–2014.
- 54 L. F. Greenlee, F. Testa, D. F. Lawler, B. D. Freeman and P. Moulin, Effect of antiscalants on precipitation of an RO concentrate: Metals precipitated and particle characteristics for several water compositions, *Water Res.*, 2010, **44**, 2672–2684.
- 55 E. L. Owens-Bennett, B. Trussell and I. Monroy, *TECHNICAL MEMORANDUM - Proposed Solids Formation Recovery Formula for the Inland Empire Brine Line*, 2016.
- 56 H. L. Yang, C. Huang and J. R. Pan, Characteristics of RO foulants in a brackish water desalination plant, *Desalination*, 2008, **220**, 353–358.
- 57 Z. Bin Xu, W. L. Wang, N. Huang, Q. Y. Wu, M. Y. Lee and H. Y. Hu, 2-Phosphonobutane-1,2,4-tricarboxylic acid (PBTCA) degradation by ozonation: Kinetics, phosphorus transformation, anti-precipitation property changes and phosphorus removal, *Water Res.*, 2019, **148**, 334–343.
- 58 L. F. Greenlee, F. Testa, D. F. Lawler, B. D. Freeman and P. Moulin, Effect of antiscalant degradation on salt precipitation and solid/liquid separation of RO concentrate, *J. Memb. Sci.*, 2011, **366**, 48–61.
- 59 K. J. Howe, A. Marwah, K. P. Chiu and S. S. Adham, Effect of membrane configuration

- on bench-scale MF and UF fouling experiments, *Water Res.*, 2007, **41**, 3842–3849.
- 60 S. S. Wadekar, T. Hayes, O. R. Lokare, D. Mittal and R. D. Vidic, Laboratory and Pilot-Scale Nanofiltration Treatment of Abandoned Mine Drainage for the Recovery of Products Suitable for Industrial Reuse, *Ind. Eng. Chem. Res.*, 2017, **56**, 7355–7364.
- 61 D. B. Mosqueda-Jimenez, R. M. Narbaitz and T. Matsuura, Membrane fouling test: Apparatus evaluation, *J. Environ. Eng.*, 2004, **130**, 90–99.
- 62 C. Liang, C. F. Huang, N. Mohanty and R. M. Kurakalva, A rapid spectrophotometric determination of persulfate anion in ISCO, *Chemosphere*, 2008, **73**, 1540–1543.
- 63 American Public Health Association, American Water Works Association and Water Environment Foundation, *Standard methods for the examination of water and wastewater*, American Public Health Association; American Water Works Association; Water Environment Foundation, 23rd Ed., 2017.
- 64 W. Li, T. Jain, K. Ishida and H. Liu, A mechanistic understanding of the degradation of trace organic contaminants by UV/hydrogen peroxide, UV/persulfate and UV/free chlorine for water reuse, *Environ. Sci. Water Res. Technol.*, 2017, **3**, 128–138.
- 65 P. Neta, R. E. Huie and A. B. Ross, Rate Constants for Reactions of Aliphatic Carbon-Centered Radicals in Aqueous Solution., *Natl. Bur. Stand. Natl. Stand. Ref. Data Ser.*
- 66 Z. Wang, Y. Shao, N. Gao, X. Lu and N. An, Degradation of diethyl phthalate (DEP) by UV/persulfate: An experiment and simulation study of contributions by hydroxyl and sulfate radicals, *Chemosphere*, 2018, **193**, 602–610.
- 67 G. V. Buxton, C. L. Greenstock, W. P. Helman and A. B. Ross, Critical Review of rate constants for reactions of hydrated electrons, hydrogen atoms and hydroxyl radicals ( $\cdot\text{OH}/\cdot\text{O}$ —in Aqueous Solution, *J. Phys. Chem. Ref. Data*, 1988, **17**, 513–886.

- 68 X. Y. Yu, Z.-C. Bao and J. R. Barker, Free Radical Reactions Involving Cl $\cdot$ , Cl $_2\cdot^-$ , and So $_4\cdot^-$  in the 248 nm Photolysis of Aqueous Solutions Containing S $_2$ O $_8^{2-}$  and Cl $^-$ , *J. Phys. Chem. A*, 2004, **108**, 295–308.
- 69 M. M. Benjamin, *Water chemistry*, Waveland Press, Inc, 2nd ed., 2014.
- 70 Y. P. Lin and P. C. Singer, Inhibition of calcite crystal growth by polyphosphates, *Water Res.*, 2005, **39**, 4835–4843.
- 71 M. M. Reddy and A. R. Hoch, Calcite crystal growth rate inhibition by polycarboxylic acids, *J. Colloid Interface Sci.*, 2001, **235**, 365–370.
- 72 Hydranautics, Chemical Pretreatment For RO and NF, <https://membranes.com/wp-content/uploads/2017/06/TAB-111.pdf>, (accessed 27 March 2020).